

Electronic and structural properties of $\text{La}_3\text{Ni}_2\text{B}_2\text{N}_3$

David J. Singh and Warren E. Pickett

Complex Systems Theory Branch, Naval Research Laboratory, Washington, D.C. 20375

(Received 21 December 1994)

$\text{La}_3\text{Ni}_2\text{B}_2\text{N}_3$ is determined, using local-density-approximation calculations, to be a three-dimensional metal, similar to $\text{LuNi}_2\text{B}_2\text{C}$ and related borocarbides. The band structure shows four hybridized bands crossing the Fermi energy, E_F . The Fermi-surface velocities in the x and z directions are 2.9×10^7 cm/s and 1.5×10^7 cm/s, respectively, i.e., a 2:1 ratio. This three-dimensional character is due to the open-shell character of the La ions and resulting participation of La orbitals in the states at E_F . The dominant La contribution at E_F comes from La $5d$ orbitals, particularly for the outer La layers; La $4f$ contributions are weaker, but significant. There is a pronounced peak in the density of states occurring near E_F due to a flat band, though this peak is somewhat smeared on the high-energy side as compared to the corresponding peak in $\text{LuNi}_2\text{B}_2\text{C}$. Internal structural coordinates and the corresponding optical Raman phonon frequencies have been calculated using force methods.

The discovery of superconductivity in Ni, Pd, and Pt rare-earth borocarbides, with critical temperatures, T_c as high as 23 K has renewed interest in superconducting intermetallics.¹⁻⁴ In particular, the rapid discovery of T_c essentially tying the record high T_c for an intermetallic, the presence of elements frequently associated with magnetism, and the anisotropic, layered crystal structures, all suggested that the superconductivity might be unconventional in analogy with the high T_c cuprates. This then leads to the expectation that much higher values of T_c may yet be discovered in these or related compounds.

Electronic structure calculations⁵⁻⁹ have, however, shown that despite the layered structures the materials have many similarities to previous families of intermetallic superconductors. Particularly striking is the fact that although the crystal structures are apparently very anisotropic, the electronic structure near the Fermi energy, E_F , is dominated by quite three-dimensional bands with nearly isotropic Fermi surface properties. Based on this as well as evidence for strong electron phonon couplings and other features analogous to older families of materials, such as a high electronic density of states (DOS) at E_F , $N(E_F)$, it has been concluded that the materials are just conventional strong coupling superconductors, and that as a result it is unlikely that T_c 's much higher than the old record of 23 K will be discovered in these compounds.

Recently, however, Cava *et al.*¹⁰ have reported superconductivity with a critical temperature of 12–13 K in an apparently related intermetallic, $\text{La}_3\text{Ni}_2\text{B}_2\text{N}_3$, with a crystal structure much more suggestive of two-dimensional behavior. In particular, like $\text{YNi}_2\text{B}_2\text{C}$, which has the highest T_c , the crystal structure contains Ni-B sheets consisting of coplanar Ni atoms closely coordinated by B atoms lying above and below the layer. In $\text{YNi}_2\text{B}_2\text{C}$ and the other materials in the family these Ni-B sheets are separated by a single Y (or other trivalent metal) carbide layer. The three dimensionality of the electronic structure near E_F is due to coupling through these Y-C layers. In $\text{La}_3\text{Ni}_2\text{B}_2\text{N}_3$, this layer is replaced by three rock salt La-N layers. This has led to the expectation of a strongly two-dimensional electronic structure, first of all due

to the larger separation between the Ni-B sheets, and second because of the likelihood that the rocksalt La-N trilayers between them are ionic and insulating or nearly insulating.¹¹ This expectation is, however, open to question, since the superconductivity in these materials is thought to be related to a peak in the electronic DOS near E_F ;⁵⁻⁸ insulating LaN is expected to have a net charge close to zero, presumably giving a different band filling and DOS peak position than a YC or LaC layer. Further, it has been shown⁶ for $\text{LuNi}_2\text{B}_2\text{C}$, that the peak structure near E_F does not occur for an isolated Ni-B sheet, but is dependent on interactions involving the Lu and C atoms as well. In the discussion that follows, we use $\text{LuNi}_2\text{B}_2\text{C}$ as an example of this family of borocarbide superconductors since its behavior seems to be generic.

Here we report density functional calculations of the electronic structure of $\text{La}_3\text{Ni}_2\text{B}_2\text{N}_3$ elucidating the relationship of this material with the borocarbide superconductors. We find the unexpected result that the LaN layers are metallic with open shell La atoms and that as a result $\text{La}_3\text{Ni}_2\text{B}_2\text{N}_3$ is quite three dimensional. In order to perform these calculations it was necessary to relax the three, presently unknown, internal structural parameters, using total energy and force methods. This also yielded the three corresponding Γ point Raman phonon frequencies.

The calculations were performed self-consistently, within the local density approximation (LDA), as parametrized by Hedin and Lundqvist¹² using the general potential linearized augmented planewave (LAPW) method.^{13,14} Well converged basis sets consisting of approximately 2025 functions were used.¹⁵ The zone integrations were based on a set of 20 special points in the irreducible wedge during the iterations to self-consistency. For the density of states (DOS), 77 points in the wedge were used. The high lying extended La $5p$ and $5s$ states were treated as valence states using a local orbital extension.¹⁶ The Raman frequencies and internal structural parameters, corresponding to the B and outer layer La and N heights, were computed from the variation of the atomic forces with structure. These forces were determined using the method of Yu, Singh, and Krakauer.¹⁷ The lattice parameters were fixed at their experimental values.

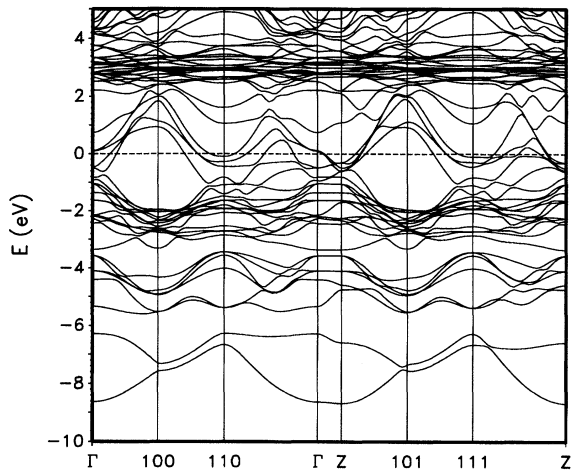


FIG. 1. Band structure of $\text{La}_3\text{Ni}_2\text{B}_2\text{N}_3$ along representative directions. Z denotes the point $(0,0,2\pi/c)$, while XYZ denotes $(X\pi/a, Y\pi/a, 2Z\pi/c)$. 110 is the X point and 100 is the D point. The dashed horizontal line denotes E_F . Although generally not symmetry directions in the body centered tetragonal zone, the lines shown are all in the plane of the layers with the exception of the Γ - Z line, which is perpendicular to this plane. The dispersion along Γ - Z as well as differences between the Γ -100-110- Γ and Z -101-111- Z panels are indicative of three-dimensional character near E_F .

The heights of the B and outer La and N atoms were found to be $z_B=0.199$, $z_{\text{La}}=0.131$, and $z_N=0.128$ in units of the c lattice parameter (20.516 \AA) and with the inner La-N layer at $z=0$.¹⁸ The calculated fully symmetric A_{1g} Raman vibrations are an almost pure La mode at 106 cm^{-1} , and two strongly mixed B,N modes at 323 cm^{-1} and 896 cm^{-1} where the upper mode has adjacent B and N atoms moving against each other. Both of these modes produce distortions of the NiB_4 tetrahedra similar to those of the A_{1g} mode in $\text{LuNi}_2\text{B}_2\text{C}$. Mattheiss, Siegrist, and Cava⁸ have suggested that the superconductivity in the borocarbides is due to a strong coupling of such modes to electrons at the Fermi energy. The highest mode (896 cm^{-1}) is at a 5% higher frequency than the corresponding A_{1g} mode in $\text{LuNi}_2\text{B}_2\text{C}$ [calculated at 850 cm^{-1} (Ref. 6)]. This is not entirely unexpected since some increase in the highest frequency is expected due to the greater number of the degrees of freedom due to outer layer N motions.

The band structure and corresponding total and atom projected DOS of $\text{La}_3\text{Ni}_2\text{B}_2\text{N}_3$ with the equilibrium atomic positions are shown in Figs. 1 and 2, respectively. Both similarities and significant differences from the electronic structure of the borocarbides are evident, but the differences seem to be more matters of detail. First of all, and perhaps most importantly, contrary to expectations of near two-dimensional character, the electronic structure near E_F derives from several bands with strong c -axis dispersions. The Fermi surface velocities, $\langle v_x^2 \rangle^{1/2}$ and $\langle v_z^2 \rangle^{1/2}$, where $\langle \rangle$ denotes an average over the Fermi surface, are $2.92 \times 10^7 \text{ cm/s}$ and $1.48 \times 10^7 \text{ cm/s}$. This gives a ratio $v_x:v_z$ of 2:1 as compared to roughly 1:1 in $\text{LuNi}_2\text{B}_2\text{C}$.⁶ The four bands that cross the Fermi energy yield large sheets of Fermi surface,

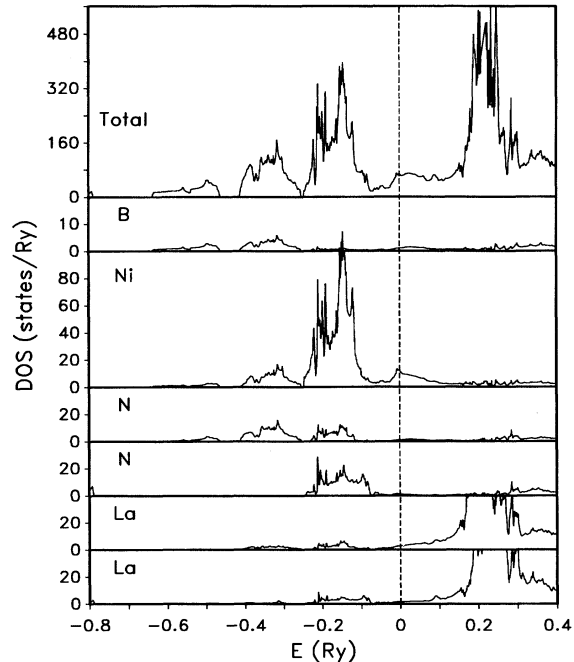


FIG. 2. Total and projected DOS of $\text{La}_3\text{Ni}_2\text{B}_2\text{N}_3$. The dashed vertical line denotes E_F . The projections are the DOS with each state, φ weighed by the integral $\int \varphi^* \varphi$ over the corresponding LAPW sphere on a per atom basis. The order of the panels (from the bottom) is (1) inner layer La, (2) outer layer La, (3) inner layer N, (4) outer layer N, (5) Ni, (6) B, and (7) the total DOS per formula unit.

as in the borocarbides; two large sheets have crossings in the c -axis direction. Thus the electronic structure of $\text{La}_3\text{Ni}_2\text{B}_2\text{N}_3$ is not in any sense two dimensional. This may be understood in terms of the DOS (Fig. 2).

The most prominent feature of the DOS about E_F is the presence of a peak, split off from the high side of the Ni d bands, similar to $\text{LuNi}_2\text{B}_2\text{C}$, for example. This peak has significant contributions from hybridization with the B atoms and also has significant contributions from the two outer La atoms, which are in proximity to the Ni-B sheets and remarkably the inner La atoms, as well. These La contributions have both $5d$ and $4f$ characters and are largest on the high-energy side of the peak, contributing to an extended tail, which is not present in $\text{LuNi}_2\text{B}_2\text{C}$. Clearly, the La atoms are open shell and only partially ionized, with the result that the La-N trilayer is metallic.

The inner layer N $1s$ core level is shifted to 0.055 Ry lower binding energy than the outer layer N $1s$ level. The inner layer La deep core levels are also shifted to lower binding energy relative to the outer La, by 0.024 Ry . This and the upward shift of the inner layer N $2p$ derived DOS all imply that the La-N layers, particularly the outer layers, have a significant net negative charge. Integration of the DOS projections gives a crude estimate of 0.5 extra electrons per outer layer.

For $\text{La}_3\text{Ni}_2\text{B}_2\text{N}_3$ ($T_c=13 \text{ K}$), we calculate $N(E_F)=57 \text{ Ry}^{-1}$ on a per formula unit basis. This may be compared with 65.3 Ry^{-1} in $\text{LuNi}_2\text{B}_2\text{C}$ ($T_c=17 \text{ K}$) (Ref. 6) and 33.9 Ry^{-1} in LaPt_2BC ($T_c=11 \text{ K}$).⁷ The Drude plasma energies,

$\hbar\Omega_{p,ii}=[4\pi e^2N(E_F)\langle v_i^2\rangle/V_c]^{1/2}$, where V_c is the cell volume, are 4.4 eV and 2.3 eV in the x and z directions, respectively. This corresponds to a BCS clean limit London penetration depth ($\Lambda=c/\Omega_p$) of 450 Å normal to c .

The main La 4*f* peaks are approximately 3 eV above E_F . At E_F the La 5*d* contribution is approximately three times larger than the La 4*f* contribution for the outer La atoms, but these are roughly equal for the inner La atom due to a smaller 5*d* contribution. The N 2*p* contributions to $N(E_F)$ are significant and arise from both the inner and outer layer N atoms; the inner N atom has only a slightly lower contribution than an outer layer N. However, besides the La-N interactions that this implies, there are strong covalent interactions both between the Ni and B atoms and between the outer N and Ni atoms as evidenced by the similar shape of their DOS projections from -0.6 to -0.2 Ry relative to E_F as well as above the La 4*f* peak. The inner layer N atoms have a much more compact 2*p* DOS reflecting the absence of Ni neighbors.

As mentioned, Mattheiss, Siegrist, and Cava⁸ have associated the superconductivity of the borocarbides with the presence of a flat band near E_F , which gives rise to the DOS peak and changes in its occupation due to strong A_{1g} phonon coupling with s - p derived bands also near the Fermi energy. The coupling is ascribed to modulation of bond angles in the NiB₄ tetrahedra. In LuNi₂B₂C this flat Ni *d* derived band is just above E_F along most of the Γ -110 line (see the caption of Fig. 1). In La₃Ni₂B₂N₃ a similar flat band occurs, but it is shifted to 300 meV below E_F along Γ -110 and acquires a considerably larger dispersion along this line. The flat Ni *d* derived section that gives rise to the DOS peak occurs rather along almost the whole Z -111 line.

As in LuNi₂B₂C, there are also predominantly s - p derived bands near the Fermi energy in La₃Ni₂B₂N₃. Examples are the two bands that disperse upwards through E_F along Γ -100, originating from Γ as a doubly degenerate state at -0.5 eV. This band at Γ is predominantly B 2*p* and outer layer N 2*p* derived. It also has La 5*d* character involving both the inner and outer layer La atoms, as well as some Ni 3*d* character. We have investigated the coupling of A_{1g} phonons to this state by calculating the electronic structure including B displacements of 0.04 Å (with additional outer

layer N displacements) as in the 323 cm⁻¹ and 896 cm⁻¹ modes.¹⁹ These involve the same distortion of the NiB₄ tetrahedra, but different modulations of the B-N and Ni-N bonds. For the higher frequency mode, this Γ point s - p band is shifted relative to E_F by 0.01 Ry (downwards for B motion towards the Ni), corresponding to a “deformation potential” of about 3 eV/Å. Similar, but generally smaller effects on the s - p bands near E_F occur throughout the zone. This is about half of the maximum value found by Mattheiss, Siegrist, and Cava⁸ for LuNi₂B₂C.

On the other hand, with displacements corresponding to the 323 cm⁻¹ mode, we find much smaller deformation potentials. For the actual crystal structure, the DOS peak near E_F occurs at -29 meV (relative to E_F). With the frozen in 896 cm⁻¹ pattern (0.04 Å), it occurs at $+99$ meV (i.e., a shift of 128 meV), while with the 323 cm⁻¹ pattern (0.04 Å) it occurs at -27 meV (shift of 2 meV). As mentioned, both the 323 cm⁻¹ and 896 cm⁻¹ modes involve the same distortion of the NiB₄ tetrahedra; the main difference is that the 896 cm⁻¹ mode modulates the outer layer N-B bond lengths, while the 323 cm⁻¹ mode does not since it involves in phase motions of the adjacent B and N atoms. (Note also that the phase of the outer layer N-Ni motions and Ni-B motions is shifted by π .) Thus the coupling of these optical phonons is due to modulation of B-N bond lengths as opposed to angles in the NiB₄ tetrahedra.

In summary, we find that La₃Ni₂B₂N₃ fits in very well with the picture provided by previous calculations for the borocarbide superconductors like LuNi₂B₂C, and should be regarded as just another member of this class. In particular, there is no near two dimensionality of the electronic structure evident near E_F . The implication is that while this and other modifications of the borocarbide superconductors may be very important in tailoring their properties, such changes are unlikely to lead to dramatically higher critical temperatures, as in the high critical temperature cuprates.

We are grateful to R. Yu for several discussions regarding LAPW forces and numerical codes to calculate them and to L. F. Mattheiss for a critical reading. Work at the Naval Research Laboratory was supported in part by the Office of Naval Research. Computations were performed using the DoD computer facilities at CEWES and NAVO.

¹R. Nagarajan, C. Mazumdar, Z. Hossain, S. K. Dhar, K. V. Golpkrishnan, L. C. Gupta, C. Godart, B. D. Padalia, and R. Vijayaraghavan, Phys. Rev. Lett. **72**, 274 (1994).

²R. J. Cava, H. Takagi, B. Batlogg, H. W. Zandbergen, J. J. Krajewski, W. F. Peck, Jr., R. B. van Dover, R. J. Felder, T. Siegrist, K. Mizuhashi, J. O. Lee, H. Eisaki, S. A. Carter, and S. Uchida, Nature (London) **367**, 146 (1994).

³R. J. Cava, H. Takagi, H. W. Zandbergen, J. J. Krajewski, W. F. Peck, Jr., T. Siegrist, B. Batlogg, R. B. van Dover, R. J. Felder, K. Mizuhashi, J. O. Lee, H. Eisaki, and S. Uchida, Nature (London) **367**, 252 (1994).

⁴R. J. Cava, B. Batlogg, T. Siegrist, J. J. Krajewski, W. F. Peck, Jr., S. Carter, R. J. Felder, H. Takagi, and R. B. van Dover, Phys. Rev. B **49**, 12 384 (1994).

⁵L. F. Mattheiss, Phys. Rev. B **49**, 13 279 (1994).

⁶W. E. Pickett and D. J. Singh, Phys. Rev. Lett. **72**, 3702 (1994).

⁷D. J. Singh, Phys. Rev. B **50**, 6486 (1994).

⁸L. F. Mattheiss, T. Siegrist, and R. J. Cava, Solid State Commun. **91**, 587 (1994).

⁹M. S. Golden, M. Knupfer, M. Kielwein, M. Buchgeister, J. Fink, D. Teehan, W. E. Pickett, and D. J. Singh, Europhys. Lett. **28**, 369 (1994).

¹⁰R. J. Cava, H. W. Zandbergen, B. Batlogg, H. Eisaki, H. Takagi, J. J. Krajewski, W. F. Peck, Jr., E. M. Gyorgy, and S. Uchida, Nature (London) **372**, 245 (1994).

¹¹G. L. Olcese, J. Phys. F **9**, 569 (1979).

¹²L. Hedin and B. I. Lundqvist, J. Phys. C **4**, 2064 (1971).

¹³O. K. Andersen, Phys. Rev. B **12**, 3060 (1975).

¹⁴S. H. Wei and H. Krakauer, Phys. Rev. Lett. **55**, 1200 (1985); D. J. Singh, *Planewaves, Pseudopotentials and the LAPW Method*

(Kluwer Academic, Boston, 1994), and references therein.

- ¹⁵ LAPW sphere radii of 2.2, 1.9, 1.3, and 1.3 a.u. were used for La, Ni, N, and B, respectively.
- ¹⁶ D. Singh, Phys. Rev. B **43**, 6388 (1991).
- ¹⁷ R. Yu, D. Singh, and H. Krakauer, Phys. Rev. B **43**, 6411 (1991).
- ¹⁸ Due to the body centering and inversion center, atoms occur at heights $\pm z$ and $0.5 \pm z$.
- ¹⁹ In order to simplify the analysis of the electron phonon coupling, idealized patterns for the upper two modes were used. These

consisted, for the 323 cm^{-1} mode of equal in-phase displacements of adjacent B and N atoms, and for the 896 cm^{-1} mode of equal out-of-phase displacements. The calculated phonon polarization vectors (order: La,N,B) are $(0.99, -0.10, -0.08)$, $(-0.13, 0.69, 0.72)$, and $(-0.02, 0.72, -0.69)$ in order of increasing frequency. Taking the masses into account, the actual ratios of N to B displacements in the upper two modes are 0.8 and -0.9 for the upper two modes.